ANALYSIS AND OPTIMIZATION FOR OFF-DESIGN PERFORMANCE OF THE RECOMPRESSION sCO2 CYCLES FOR HIGH TEMPERATURE CSP APPLICATIONS

Louis A. Tse
Department of Mechanical and Aerospace Engineering
University of California, Los Angeles
Los Angeles, CA, USA

Ty Neises
National Renewable Energy Laboratory
Golden, CO 80401

Louis Tse is a Ph.D. candidate at the UCLA Department of Mechanical and Aerospace Engineering. He was awarded the NSF Graduate Research Fellowship in 2012 for research of a novel thermal energy storage (TES) system funded by the Department of Energy. His specialization includes numerical modeling, non-linear optimization, heat transfer, and systems engineering. Louis completed his B.S. in Mechanical Engineering from Arizona State University with Summa Cum Laude honors.

Ty Neises joined the Thermal Systems group at NREL in 2011. His work focuses on modeling and analyzing the thermal fluid performance of concentrating solar power (CSP) systems and components. His recent work includes researching supercritical carbon dioxide (sCO2) systems for CSP applications and supporting the design of a high-pressure power tower receiver. Ty also develops and supports models for the System Advisor Model.

ABSTRACT
This study investigates optimal design and operation of supercritical carbon dioxide (sCO2) power cycles for concentrating solar power (CSP) applications. Previous design-point and off-design studies have supported the potential efficiency improvements and established broad operating conditions for the sCO2 power cycle at temperatures pertinent to CSP applications. This study investigates a simple/recompression sCO2 cycle integrated with molten salt heat source and maximizes cycle efficiency for off-design operation. The findings of this study report optimal operating parameters under off-design conditions and provide an understanding of the effect of cycle parameters on other primary subsystems in a CSP plant.

INTRODUCTION
Concentrating solar power utilizes solar beam irradiance to produce heat for a thermodynamic power cycle. Consequently, CSP employs power cycle concepts similar to those found in coal and nuclear power plants. Previous studies have suggested that the sCO2 power cycle has the potential to replace the steam-Rankine cycle for at least some CSP configurations [1-4]. Researchers in fossil, nuclear, waste heat, and other application spaces have studied cycle component design and manufacturing and cycle design and operation. This research informs the CSP community about the cycle; however, CSP presents its own unique challenges in designing and operating a power cycle.

One typical CSP system configuration is to capture the solar heat with a fluid that can be stored. Typically the storage fluid stores the thermal energy over a temperature gradient. As such, the volume of fluid required is proportional to the temperature gradient of the cycle's heat input. Therefore, all else equal, design and operation strategies that create a larger temperature gradient are preferred. Thermal storage allows the plant operator to decide when to dispatch the stored, hot fluid to the power cycle to generate electricity. This capability allows CSP plants to increase revenue potential by generating electricity during peak demand, with these peak pricing periods often coincide with hot, summer afternoons. Furthermore, locations with the best solar resource typically prohibit evaporative cooling. Therefore, it is paramount that the power cycle is designed to achieve high performance with hot compressor inlet temperatures. Additionally, some CSP design and operation strategies require that part-load operation is understood.

While researchers are interested in the sCO2 concept for both CSP and traditional heat sources, CSP and nuclear power cycle configurations differ from coal and natural gas cycles in that the heat source is a heat flux instead of a sensible heat source (i.e. waste heat and combustion gas heating). The result of this difference is that CSP and nuclear sCO2 cycles are designed to limit the temperature range at which thermal energy is injected to the cycle, with a general goal to balance a hot average injection temperature with a reasonable power density. Two of the most common cycle configurations for flux based applications are shown in Figure 1. The simple, recuperated cycle (a) is the least complex but least efficient configuration. Many publications detail the benefit of adding a recompressor (b) to the simple cycle. Essentially, the recompressor facilitates more effective heat exchange in the low-temperature recuperator, resulting in better recuperation and a more efficient cycle. The trade-off is that the recompressor consumes work from cycle. While research at NREL and other institutions has suggested that the partial cooling cycle may offer additional benefits over the recompression cycle [1], this paper focuses on the recompression cycle because it is the most likely near-term, high efficiency solution.
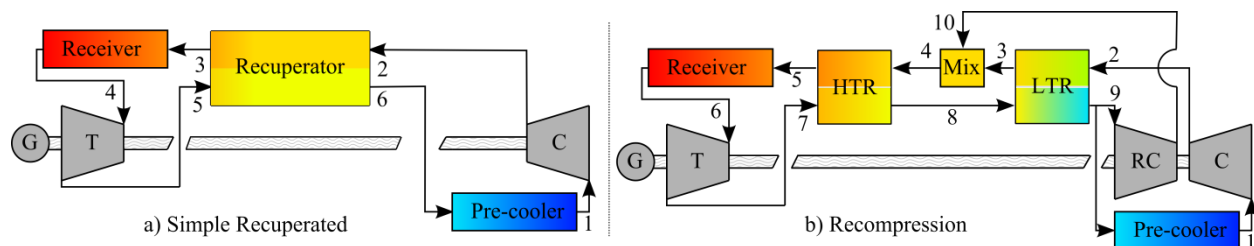
Figure 1: Common sCO2 cycle configurations for flux based heat sources.

Dyreby [5] presented an extensive investigation of the off-design performance of the simple and recompression cycles. The study assumed a generic heat input into the cycle to stay relevant to all applications. The analysis studied several cycle designs. One primary design choice studied was the design-point compressor inlet temperature, which subsequently influences recuperator conductance, turbomachinery sizing, and thermal efficiency. The study strongly suggests that for power cycles expected to operate under off-design conditions, as would be the case for CSP applications, a relatively hot compressor inlet temperature is preferred, especially when considering simple cycles. On the other hand, the study shows that the low-temperature compressor inlet recompression design can be advantageous if the cycle will rarely experience

off-design operation. This could occur for applications with a fairly consistent heat sink, e.g. a large body of water utilized for once-through cooling.

This study builds on Dyreby's work by integrating his model with a hot molten salt heat source. This extension enables analysis of issues unique to CSP. Specifically, this study varies the off-design compressor inlet temperature and molten salt mass flow rate and temperature to investigate: 1) cycle design and off-design performance when the heat input source and heat exchanger are defined, 2) the potential impact on molten salt cold return temperature when off-design performance is optimized, and 3) estimated annual efficiencies for two different design compressor inlet temperatures.

MODELING APPROACH

This study uses two design point and two off-design models to generate results of a sCO2 recompression cycle configured for CSP applications. As such it's important to document each model's input parameters, solution, and interaction with other models. Figure 2 shows this information at a high level and differentiates between *cycle* models developed by Dyreby [5] and *application* models we developed for CSP analysis. The following subsections provide more detail for each model, with a focus on the *application* modeling additions.
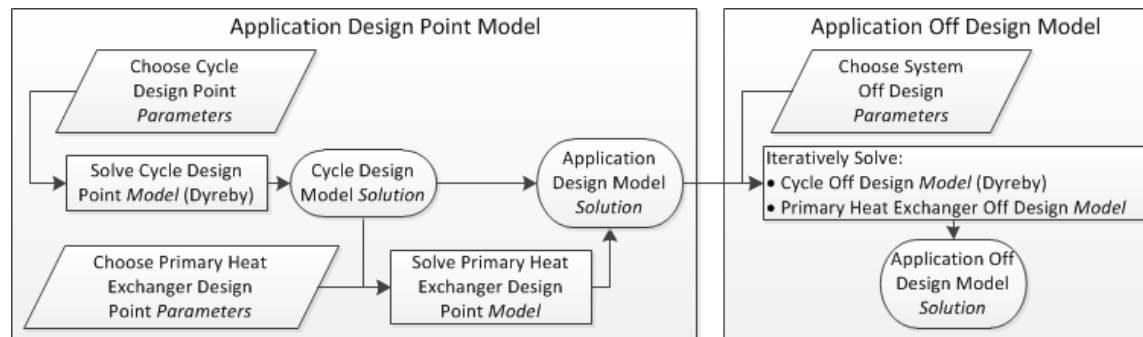
Figure 2: Modeling information flow diagram for the design point and off design models.

Cycle Design Point Model

The cycle design point model uses equipment and operational parameters to find the combination of compressor inlet pressure, pressure ratio, and recompression fraction that results in the smallest recuperator conductance while still achieving the target cycle thermal efficiency. The model then uses this information to size the turbomachinery. More detailed description of this model is provided by Dyreby [5]. Table 1 describes the parameters and solution values, with numbers from our baseline case.

The compressors and turbine all have independent shafts in this configuration. The turbine shaft speed is fixed to 3,600 rpm for a grid-connected synchronous generator. The model assumes that the shaft speed of each compressor is independently adjustable.

Table 1: Cycle design point model parameters and solution results. Numbers in this table represent the design used in the following discussion.

Design Point Parameters	Optimized Design Point Parameters

3

Net Power Output	10	MW	Comp. Inlet Pressure	9.00	MPa
Thermal Efficiency (no cooling)	0.48	-	Comp. Pressure Ratio	2.74	-
Turb. Inlet Temp	690	°C	Recompression Fraction	0.18	-
Turb. Isentropic Efficiency	0.93	-	**Design Point Solution Results**		
Turb. Shaft Speed (fixed)	3600	rpm	Recuperator Conductance	1375	kW/K
Main Comp. Inlet Temp	45	°C	PHX NTU	9.39	
Comp. Isentropic Efficiency	0.89	-	Main Comp. Shaft Speed	33294	rpm
Maximum Pressure	25	MPa	Turb. Rotor Diameter	2.32	m
Neglecting Pressure Drops			CO2 Mass Flow Rate	82.0	kg/s
			PHX CO2 Inlet Temperature	505	°C

Cycle Off-Design Model

The cycle off-design model uses design point solution results that describe component design to predict the cycle performance when the off-design parameters vary from their design values. For example, the off-design compressor uses the design compressor rotor diameter and design efficiency along off-design parameters compressor shaft speed and compressor inlet temperature to calculate the compressor outlet pressure, isentropic efficiency, and power consumption. As with the cycle design point model, Dyreby [5] provides a more detailed description of this model. Table 2 lists the required cycle design point solution results, parameters, and results for the off-design model. The off-design model optimizes the compressor shaft speed, main compressor inlet pressure, and the recompression fraction off-design parameters to maximize the cycle thermal efficiency.

Table 2: Cycle off-design model required design point solution results, parameters, and solution results. Numbers in this table are selected from the off-design analysis presented in the following discussion.

Required Design Point Solution Results	Off-Design Parameters		Off-Design Results		
Recuperator Conductance	Turb. Inlet Temp	687 °C	Net Power Output	9.30	MW
Turb Isen Efficiency	Comp. Inlet Temp	50 °C	Thermal Efficiency	0.47	-
Turb. Rotor Diameter	**Optimized Off-Design Parameters**		PHX CO2 Inlet Temp.	510	°C
Comp. Isen Efficiency (2)	Main Compressor Shaft Speed	36523 rpm	Pressure Ratio	2.73	-
Comp. Rotor Diameter (2)	Main Compressor Inlet Pressure	9.0 MPa	CO2 Mass Flow Rate	82.9	kg/s
Maximum Pressure	Recomp. Fraction	0.17 -			
Component Pressure Drops					

Primary Heat Exchanger Design Point Model

We are modeling the primary heat exchanger as a counter-flow molten salt to CO2 heat exchanger. The goal of the design point model is to use information from the cycle design point solution and the molten salt hot inlet temperature to calculate the required conductance (UA) of

the primary heat exchanger. We set the capacitance ratio (CR) at design to 1.0, thereby ensuring that the molten salt and CO2 streams both experience the same inlet-to-outlet temperature differential. Then, we calculate the maximum possible heat transfer in the heat exchanger using Equation (1). Next, we find the heat exchanger effectiveness (ε) by dividing the actual heat transfer by the maximum heat transfer. Finally, we calculate the UA using Equation (2).

$$\dot{q}_{max} = \left(\dot{m}cp\right)_{CO_2,des} \cdot \left(T_{HTF,hot} - T_{CO_2,PHX,in}\right) \tag{1}$$

$$UA_{des} = \frac{\varepsilon}{1-\varepsilon}\left(\dot{m}cp\right)_{CO_2,des} \tag{2}$$

Table 3 shows the required *cycle* design point solution results, the primary heat exchanger design point parameters, and the primary heat exchanger design point solution results. Note that one outcome of fixing the CR is that the design heat transfer fluid (HTF) mass flow rate is a *dependent* variable calculated by the primary heat exchanger design point model, while the HTF temperature is a design parameter. Alternatively, we could specify the HTF mass flow rate and let the CR vary, but that allows for the potential of a significantly unbalanced heat exchanger that could result in suboptimal *application* design. Ultimately, the optimal CR is a function of heat exchanger and system costs and performance, and is outside the scope of this paper.

Table 3: Primary heat exchanger model required *cycle* design point solution results, design point model parameters, and solution results. Numbers in this table represent the design used in the following discussion.

Required Design Point Solution Results	Design Point Parameters		Design Point Solution Results		
PHX CO2 Inlet Temperature	HTF Inlet Temp	700 °C	PHX Conductance	2.9×10^5	kW/K
Turb. Inlet Temp			PHX NTU	9.39	
CO2 Mass Flow Rate			HTF Mass Flow Rate	72.4	kg/s

Primary Heat Exchanger Off-Design Model
During off-design operation, we know the cold CO2 inlet and hot HTF inlet temperatures and mass flow rates, and we want to solve for the outlet temperature of both streams. Because both the mass flow rates can be different than their respective design point values, the convective heat transfer coefficient, and therefore the conductance, of the heat exchanger can vary. We estimate the off-design overall heat transfer coefficient, *U*, using Equation (3), based upon the Dittus-Boelter correlation for the effect of mass flow rate on heat transfer coefficient (Patnode [6]). Next, we calculate the off-design capacitance ratio using Equation (4). Then, we apply Equation (5) to find the NTU. Next, we find the off-design effectiveness using Equation (6). Finally, Equation (7) uses the effectiveness to calculate the off-design heat transfer, which we use to calculate the outlet temperatures. Table 4 lists the required *PHX* design point solution results, required *cycle* off-design solution results, parameters, and results for the PHX off-design model.

$$U = U_{des} \left(\frac{1}{2} \left(\frac{\dot{m}_{CO_2}}{\dot{m}_{CO_2,des}} + \frac{\dot{m}_{HTF}}{\dot{m}_{HTF,des}} \right) \right)^{0.8} \tag{3}$$

$$C_R = \frac{\dot{C}_{min}}{\dot{C}_{max}} = \frac{\min\left(\left[(\dot{m}c_p)_{CO_2} \right], \left[(\dot{m}c_p)_{HTF} \right] \right)}{\max\left(\left[(\dot{m}c_p)_{CO_2} \right], \left[(\dot{m}c_p)_{HTF} \right] \right)} \tag{4}$$

$$NTU = \frac{UA}{\dot{C}_{min}} \tag{5}$$

$$\varepsilon = \begin{cases} \dfrac{1 - \exp\left(-NTU\left(1 - C_R\right)\right)}{1 - C_R \exp\left(-NTU\left(1 - C_R\right)\right)}, & \left(for\ C_R < 1.0 \right) \\[4mm] \dfrac{NTU}{1 + NTU}, & \left(for\ C_R \geq 1.0 \right) \end{cases} \tag{6}$$

$$\dot{Q}_{PHX} = \varepsilon \dot{C}_{min} \left(T_{HTF,hot} - T_{CO_2,PHX,in} \right) \tag{7}$$

Table 4: Primary heat exchanger off-design model required *PHX* design point solution results, required *cycle* off-design solution results, off-design parameters, and off-design results. Numbers in this table are selected from the off-design analysis presented in the following discussion.

Required *PHX* Design Point Solution Results	Required *Cycle* Off-Design Solution Results		Off-Design Results	
PHX Conductance	PHX CO2 Inlet Temp.	510 °C	Turb. Inlet Temp	687 °C
HTF Mass Flow Rate	CO2 Mass Flow Rate	82.9 kg/s	HTF Return Temp	520 °C
	Off-Design Parameters			
	HTF Inlet Temp	700 °C		

Solving the Application Off-Design Model

We described above that the cycle design point model is solved independently of and before the primary heat exchanger design point model, because the design of the cycle informs the design of the heat exchanger. However, Figure 2 shows that for the off-design application model, the primary heat exchanger and cycle solutions are coupled and must be solved iteratively, as illustrated in Figure 3. The turbine inlet temperature is a function of the molten salt inlet temperature and mass flow rate, and the CO2 inlet temperature and mass flow rate to the primary heat exchanger. If all other off-design parameters in Table 2 are known, then setting the turbine inlet

temperature will constrain the off-design performance. However, the off-design performance determines the CO2 inlet temperature and mass flow rate to the primary heat exchanger. Therefore the problem is iterative, and for each unique set of off-design parameters there is only one turbine inlet temperature that results in the correct primary heat exchanger behavior (i.e. calculated conductance equal to actual conductance).
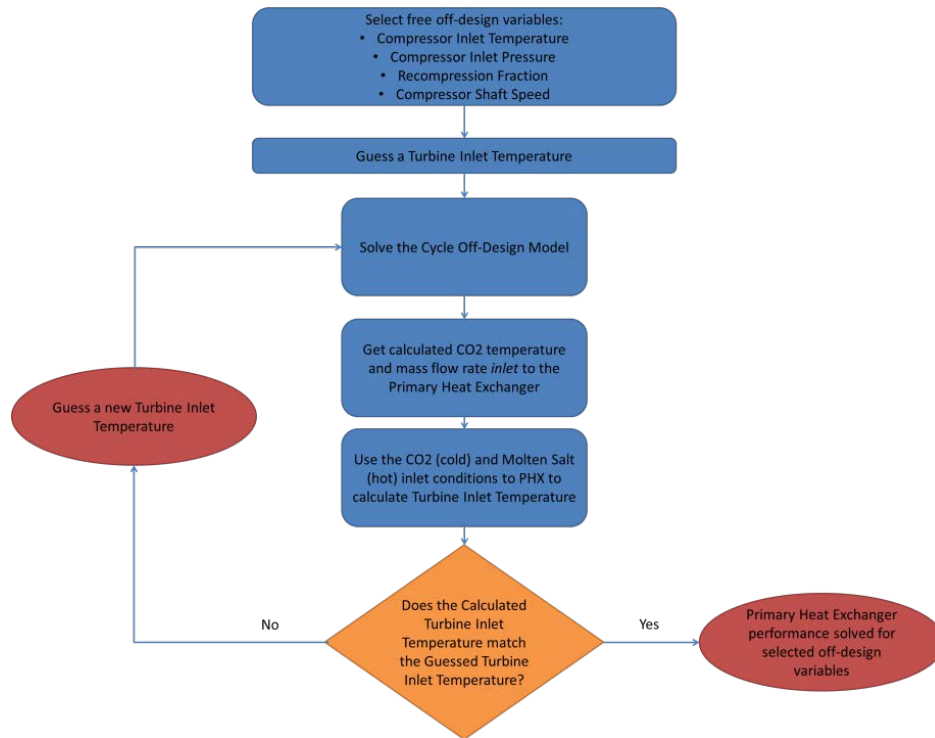
Figure 3: Information flow diagram for Primary Heat Exchanger convergence.

OFF-DESIGN PERFORMANCE ANALYSIS

To assess the integration of the sCO2 cycle into CSP applications, the inclusion of the primary heat exchanger model is necessary because it provides several important parameters. Firstly, the cycle model considers an agnostic heat source input into the CO2 stream. With the addition of the PHX model, the salt-to-CO2 approach temperature may provide an equivalent heat input to the cycle model, but at a turbine inlet temperature different from that at design, thereby affecting efficiency. Secondly, optimizing cycle efficiency with the addition of a PHX model may result in a HTF cold temperature that deviates from design-point value. Warmer HTF cold temperatures are of particular concern, as this effectively reduces thermal energy storage capacity (which is dependent upon a temperature differential), and impacts fluid flow through the receiver, and may risk venturing into unfavorable HTF property regimes.

As described in previous sections, previous studies have explored the *cycle* off-design behavior when turbine inlet temperature, heat input, and compressor inlet temperature vary. This section aims to investigate the interaction between cycle and heat exchanger parameters, and the relative magnitude of multiple parameters simultaneously experiencing off-design conditions on cycle efficiency. Table 5 describes the range of off-design conditions for each off-design parameter in

the following analysis. The cycle design point is described in Table 1 and Table 2, while an off-design example solution is shown in Table 3 and Table 4.

Table 5: Design-point values for the baseline system under study.

Primary parameter	Design-point value	Range	Secondary parameter values
$T_{htf,hot}$	700	500 – 800	$T_{mc,in} = 35, 45, 55$
$\dot{m}_{htf,frac}$	1.0	0.6 – 1.2	$T_{htf,hot} = 675, 700, 725$
$T_{mc,in}$	45	35 – 50	$\dot{m}_{htf,frac} = 0.6, 1.0, 1.2$

The results from the off-design performance analysis are shown in Figure 4. The thermal efficiency is normalized by the design-point value. Figure 4a shows that operating at warmer compressor inlet temperatures decreases thermal efficiency appreciably. It is also important to note that Dyreby's design-point analysis shows the slope of the efficiency curve is much steeper for designs with colder main compressor inlet temperature. For example, the baseline design-point value for the compressor inlet temperature is 45°C, which is relatively warm; if the system were designed for a colder compressor inlet temperature, the slope would be steeper at warmer temperatures.

Figure 4b illustrates the impact of mass flow fraction on off-design performance. As the mass flow fraction decreases to 60% of its design-point value, off-design thermal efficiency decreases by approximately 5%. Lower mass fractions essentially translate to reduced heat input into the cycle, and compressor speed and inventory control are able to compensate to a certain degree to maximize off-design thermal efficiency.

Finally, Figure 4c describes the effect of HTF hot temperature during off-design conditions, which typically occur during periods of cloud cover or nighttime, or when thermal storage is unavailable. One important observation is that for this baseline system, HTF hot temperature is the parameter with the most markedly dramatic shifts during off-design operation. Of course, one important driver of this trend is the Carnot limit. The results in Figure 4c clearly illustrate that the optimal plant operation (to maximize efficiency) must focus upon achieving design-point HTF hot temperature. In existing systems, this is achieved in a number of ways, including varying HTF mass flow rate to the solar field, implementing fossil backup or thermal storage, and increasing the solar multiple of the plant. However, this analysis does not consider the disadvantages of these plant designs which must be balanced with cycle performance.

8
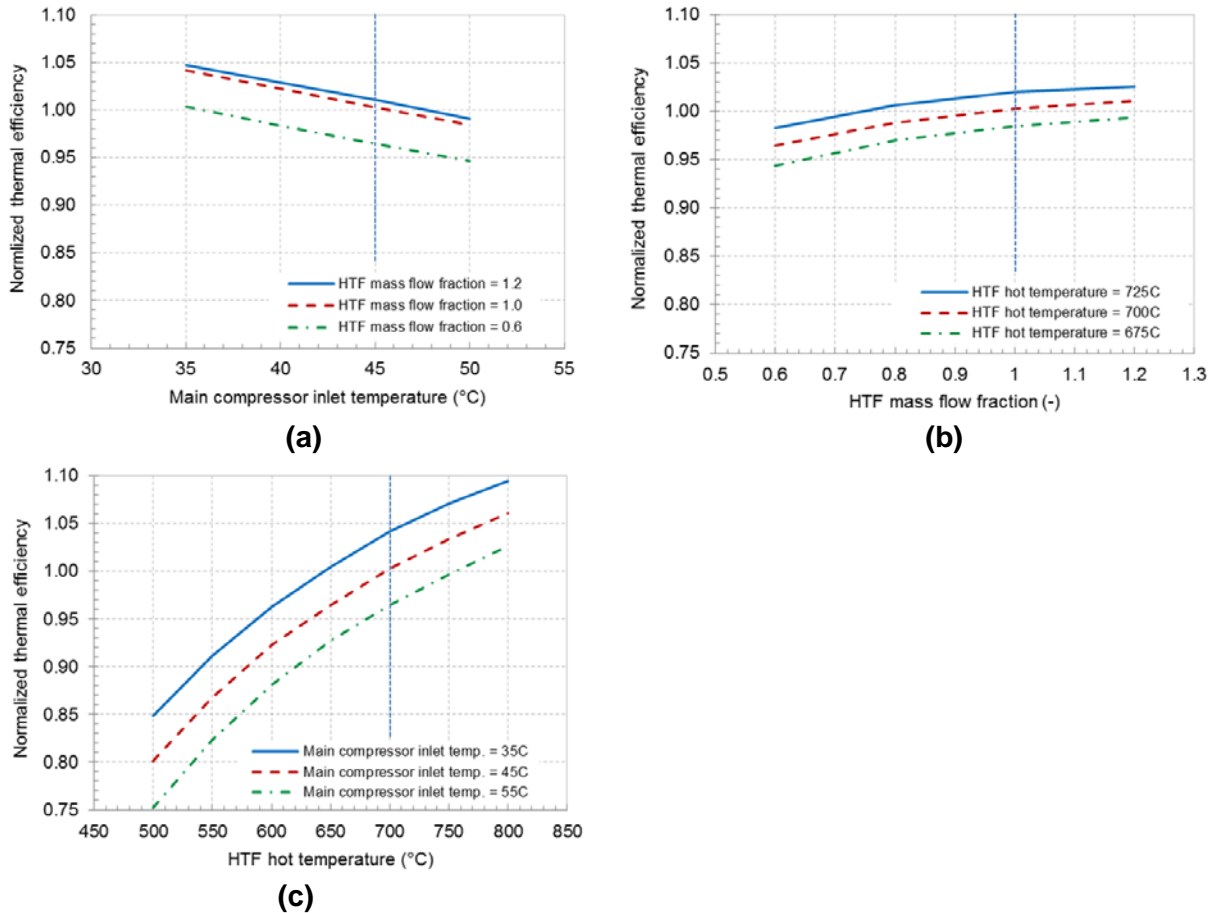
Figure 4: Design of experiments study of various off-design (OD) conditions, investigating the main and interaction effects: a) main compressor inlet temperature, b) mass flow fraction, and c) HTF hot temperature. Design-point values are given by the dashed vertical line.

Because CSP applications are expected to be dry-cooled in hot climates, off-design performance at warmer compressor temperatures is of particular interest. Further, the HTF cold temperature is also important for CSP applications because of its significance to other CSP plant components, such as the thermal storage and receiver subsystems, both of which are designed to operate for a specific temperature differential. Should the HTF cold temperature increase during off-design operation the overall storage capacity is lessened. Figure 5a shows the HTF cold temperature as a function of main compressor inlet temperature. One key observation is the HTF cold temperature increases substantially for mass flow fractions below design-point, which can occur with varying frequency depending on the plant's thermal storage capacity and operation strategy. Also important to note is that the HTF cold temperature can increase appreciably for warmer compressor inlet temperatures. Figure 5b shows the HTF temperature differential normalized to the design-point value, and suggests that storage capacity at part load is roughly 80% of the design capacity. This conclusion, along with decreased part load efficiencies, may influence the plant operation strategy to focus on full load storage dispatch to the power cycle.

(a)   **(b)**
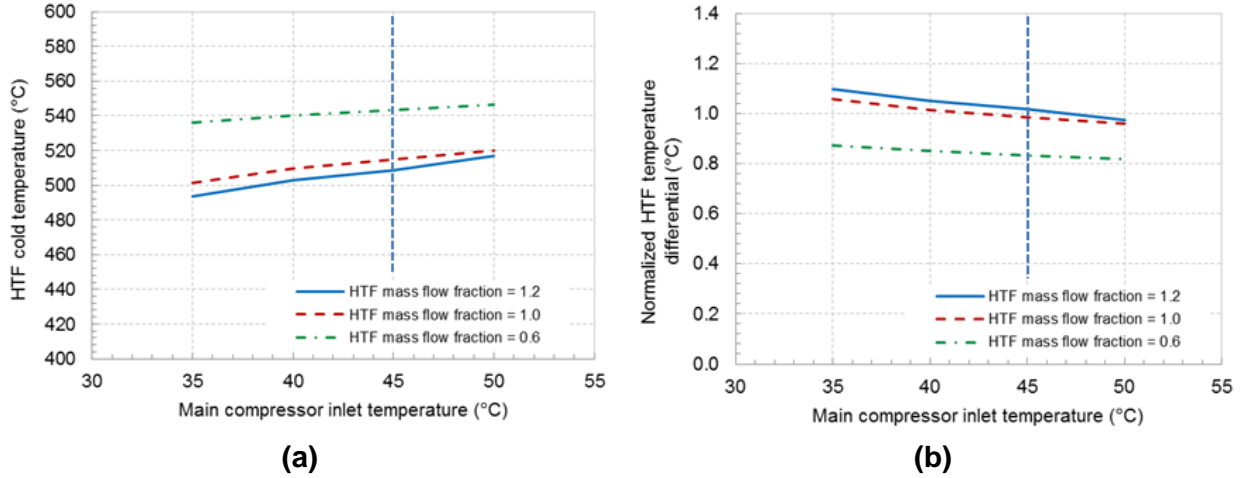
Figure 5: HTF cold temperature and normalized HTF temperature differential across the primary heat exchanger as a function of main compressor inlet temperature.

Probabilistic performance analysis

Off-design performance across an annual basis is critical to evaluating the technical and economic feasibility of the system. As shown in the previous section, main compressor inlet temperature is highly influential for off-design thermal efficiency. In this analysis, we assume that the cooling system can maintain a constant temperature differential of 15°C such that

$$T_{mc,in} = \max(T_{amb} + 15°C, \ 31°C) \tag{8}$$

with the minimum of 31°C to stay above the critical point of CO_2, and the parasitic load of the cooling fan being neglected for this study. To estimate the performance of the cycle on an annual basis, hourly DNI and ambient temperature data can be incorporated into the analysis by using a probability distribution function (PDF) to quantify the probability of achieving performance or cost targets. The PDF of the ambient temperature and DNI weighted ambient temperature compiled from the Typical Meteorological Year (TMY2) weather dataset for Daggett, CA is shown in Figure 6. The DNI weighted ambient temperature probabilities represent more realistic conditions for CSP power cycle operation, as current conventional wisdom expects CSP plants generate electricity during peak pricing periods rather than operate as baseload plants. Note that, as expected, the DNI weighted probabilities are shifted towards warmer temperatures.
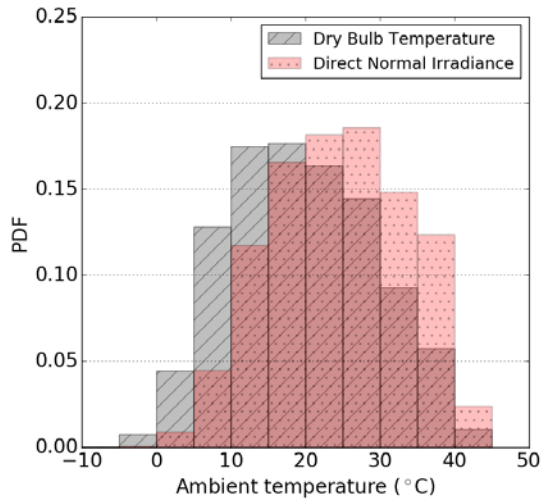
Ambient temperature (°C)	Ambient temperature-weighted probability	DNI-weighted probability
-7.5°C	0.02%	0.00%
-2.5°C	0.78%	0.05%
2.5°C	4.45%	0.87%
7.5°C	12.80%	4.50%
12.5°C	17.47%	11.72%
17.5°C	17.67%	16.54%
22.5°C	16.34%	18.17%
27.5°C	14.42%	18.55%
32.5°C	9.26%	14.83%
37.5°C	5.76%	12.35%
42.5°C	1.04%	2.42%

Figure 6: Probability density function of ambient temperature-weighted and direct normal irradiance-weighted probability, with a table of probability values located at the midpoint of each bin.

Then, based upon the probability distribution that the s-CO2 cycle will experience a variable main compressor inlet temperature throughout the year, we can assess annual performance by combining the modeled off-design efficiency at each temperature with its associated probability.

In addition to the baseline cycle design, another cycle design is considered for comparative analysis. The baseline cycle is designed for 35°C main compressor inlet temperature, which results in design values outlined in Table 1. The second cycle design being considered has a design-point of 45°C for main compressor inlet temperature. To put both designs on equal footing, they maintain the same heat exchanger thermal conductance as the baseline design. The results from this analysis are detailed in Table 6.

Table 6: Results of the probabilistic modeling for off-design main compressor inlet temperature using DNI-weighted dry-bulb temperature from Daggett, CA, where design-point efficiency is denoted with (*).

Ambient temperature (°C)	Design-point Thermal Efficiency	
	Compressor inlet temperature 35°C	Compressor inlet temperature 45°C
-10°C – 15°C	52.6%	50.6%
17.5°C	52.2%	50.3%
22.5°C	51.0%	49.4%
27.5°C	48.1%	48.6%
32.5°C	46.4%	47.7%
37.5°C	44.6%	46.8%
42.5°C	42.8%	45.9%

Annual parameters		
Ambient temperature-weighted annual efficiency (-)	50.5%	49.5%
Direct normal irradiance-weighted annual efficiency (-)	49.3%	48.9%

The results observed in Table 6 support and expand upon the results of both the design-point and off-design analysis. The system designed for 35°C compressor inlet temperature can achieve a maximum thermal efficiency of 52.6% yet drops to 42.8% during periods of high ambient temperature, while the system designed for 45°C compressor inlet temperature can achieve between 45.9%-50.6% for the same ambient temperature range. Incorporating the probability distribution for the entire year to calculate annual thermal efficiency weighted by ambient temperature or direct normal irradiance, the system designed for 35°C compressor inlet temperature achieves higher performance. However, it is clear that considering the DNI-weighted ambient temperatures resulting in the 45°C design being relatively more competitive with the 35°C design, and it is likely that a design temperature between these two points is optimal for this simplified study. Ultimately, the relationship between the value of electricity generation and ambient temperature will drive the compressor design temperature, and it is likely that paradigm will result in warmer compressor inlet temperatures than the ambient or DNI-weighted approaches.

Future work includes a wider parameter investigation during off-design operation to determine benefits and drawbacks, such as inlet compressor pressure (also known as inventory control), cooling air mass flow rate, and turbomachinery rotational speeds. Furthermore, this analysis will be extended to analyze constraining the cycle to achieve a constant HTF cold temperature and the associated tradeoffs.

CONCLUSION
This study investigates the performance of a recompression sCO2 Brayton cycle integrated with thermal storage in a CSP context, for both design-point and off-design conditions. Results of the design analysis showed that the inclusion of a HTF and primary heat exchanger model agree with previous studies suggesting that CSP plants must place careful consideration of the coupled system design parameter space, such as heat exchanger conductance, temperature differential across the heat exchanger, work output, and cycle efficiency. The performance analysis revealed the relative magnitude of the influence for two parameters both varying simultaneously off-design on cycle efficiency, HTF cold temperature, among other parameters. The current study highlights that off-design performance not only has immediate impacts on cycle efficiency, but also influences HTF cold temperature, which has indirect and important implications on thermal storage and receiver performance. Finally, approximate annual efficiency calculations suggest that expected weather conditions during cycle operation should be considered when designing the system.

BIBLIOGRAPHY

[1] Neises, T., and Turchi, C., 2014, "A comparison of supercritical carbon dioxide power cycle configurations with an emphasis on CSP applications," Energy Procedia, 49, pp. 1187-1196.

[2] Turchi, C. S., Ma, Z., Neises, T. W., and Wagner, M. J., 2013, "Thermodynamic study of advanced supercritical carbon dioxide power cycles for concentrating solar power systems," Journal of Solar Energy Engineering, 135(4), p. 041007.

[3] Chapman, D. J., and Arias, D. A., "An Assessment of the Supercritical Carbon Dioxide Cycle for Use in a Solar Parabolic Trough Power Plant," Proc. Proceedings of SCCO2 Power Cycle Symposium, RPI, Troy, NY, April, pp. 29-30.

[4] Ma, Z., and Turchi, C., "Advanced supercritical carbon dioxide power cycle configurations for use in concentrating solar power systems," Proc. Proceedings of Supercritical CO2 Power Cycle Symposium, pp. 24-25.

[5] Dyreby, J. J., 2014, "Modeling the Supercritical Carbon Dioxide Brayton Cycle with Recompression," THE UNIVERSITY OF WISCONSIN-MADISON.

[6] Patnode, A. M., 2006, "Simulation and performance evaluation of parabolic trough solar power plants," University of Wisconsin.